



OPEN ACCESS

EDITED BY

Silviya Petrova Zustiak,
Saint Louis University, United States

REVIEWED BY

Jaroslav Fojt,
University of Chemistry and Technology in
Prague, Czechia
Sharanabasava V. Ganachari,
KLE Technological University, India

*CORRESPONDENCE

Jan M. Macak,
✉ jan.macak@upce.cz
Tomas Rousar,
✉ tomas.rousar@upce.cz

RECEIVED 23 October 2024

ACCEPTED 13 November 2024

PUBLISHED 02 December 2024



CITATION

Sepúlveda M, Capek J, Baishya K,
Rodriguez-Pereira J, Bacova J, Jelinkova S,
Zazpe R, Sopha H, Rousar T and Macak JM
(2024) Enhancement of biocompatibility of
anodic nanotube structures on biomedical
Ti–6Al–4V alloy via ultrathin TiO₂ coatings.
Front. Bioeng. Biotechnol. 12:1515810.
doi: 10.3389/fbioe.2024.1515810

COPYRIGHT

© 2024 Sepúlveda, Capek, Baishya, Rodriguez-
Pereira, Bacova, Jelinkova, Zazpe, Sopha,
Rousar and Macak. This is an open-access
article distributed under the terms of the
[Creative Commons Attribution License \(CC BY\)](https://creativecommons.org/licenses/by/4.0/).
The use, distribution or reproduction in other
forums is permitted, provided the original
author(s) and the copyright owner(s) are
credited and that the original publication in this
journal is cited, in accordance with accepted
academic practice. No use, distribution or
reproduction is permitted which does not
comply with these terms.

Enhancement of biocompatibility of anodic nanotube structures on biomedical Ti–6Al–4V alloy via ultrathin TiO₂ coatings

Marcela Sepúlveda^{1,2}, Jan Capek³, Kaushik Baishya²,
Jhonatan Rodriguez-Pereira^{1,2}, Jana Bacova³,
Stepanka Jelinkova³, Raul Zazpe^{1,2}, Hanna Sopha^{1,2},
Tomas Rousar ^{3*} and Jan M. Macak ^{1,2*}

¹Center of Materials and Nanotechnologies, Faculty of Chemical Technology, University of Pardubice, Pardubice, Czechia, ²Central European Institute of Technology, Brno University of Technology, Brno, Czechia, ³Department of Biological and Biochemical Sciences, Faculty of Chemical Technology, University of Pardubice, Pardubice, Czechia

This work aims to describe the effect of the surface modification of TiO₂ nanotube (TNT) layers on Ti–6Al–4V (TiAlV) alloy by ultrathin TiO₂ coatings prepared via Atomic Layer Deposition (ALD) on the growth of MG-63 osteoblastic cells. The TNT layers with two distinctly different inner diameters, namely ~15 nm and ~50 nm, were prepared via anodic oxidation of the TiAlV alloy. Flat, i.e., non-anodized, TiAlV alloy foils were used as reference substrates. Additionally, a part of the TNT layers and alloy foils was coated with ultrathin coatings of TiO₂ by ALD. The number of TiO₂ ALD cycles used was 1 and 5 leading to a nominal TiO₂ thickness of ~0.055 and ~0.3 nm, respectively. The ultrathin TiO₂ coating by ALD enabled to optimize the surface hydrophilicity for optimal cell growth. In addition, coatings shaded impurities of V- and F-based species (stemming from the alloy and the anodization electrolyte) that affect the biocompatibility of the tested materials while preserving the original structure and morphology. The evaluation of the biocompatibility before and after TiO₂ ALD coating on TiAlV flat surfaces and TNT layers was carried out using MG-63 osteoblastic cells and compared after incubation for up to 96 h. The cell growth, adhesion, and proliferation of the MG-63 on TiAlV foils and TNT layers showed significant enhancement after the surface modification by TiO₂ ALD.

KEYWORDS

Ti–6Al–4V alloy, TiO₂ nanotube layers, atomic layer deposition, MG-63 cells, cell growth, cell proliferation

1 Introduction

Titanium (Ti) and its alloys stand out among commercially available metallic implant biomaterials, demonstrating consistent applicability attributed to their satisfactory mechanical properties, excellent biocompatibility, and corrosion resistance (Chen and Thouas, 2015; Sarraf et al., 2021). Approximately 50% of biomedical implants are manufactured using Ti–6Al–4V (TiAlV) alloy with an $\alpha + \beta$ phase composition (Singh and Dahotre, 2007). Nevertheless, the exposure of metallic implants to highly corrosive body fluids triggers corrosion processes that may negatively impact both the biocompatibility and mechanical

integrity of the implants (Oliveira et al., 2006). In addition to corrosion, metallic implants may be susceptible to other forms of degradation, including wear and tribocorrosion (Campoccia et al., 2006). These processes can lead to the release of metallic particles and/or ions, often associated with inflammatory responses and the activation of bone-resorbing cells (osteoclasts) (Vasconcelos et al., 2016; Costa et al., 2019). This avalanche of events may result in osteolysis (bone resorption) and, ultimately, implant loosening. The biological effects associated with them remain incompletely understood, and their long-term impacts cannot yet be safely predicted (Zhao and Castranova, 2011; Kontinen and Pajarinen, 2013). To prolong the effective lifetime of implant materials, it is essential to further improve the osseointegration and corrosion resistance of the exposed implant material against undesired biochemical reactions of TiAlV (Nune et al., 2018; Im et al., 2022).

Microroughness has been extensively discussed in the literature to have a beneficial effect on the osseointegration of implants (Gittens et al., 2014). This can be achieved by nanostructuring the implant's surface, leading to improved osseointegration, corrosion resistance, and longevity of the implants (Magesh et al., 2018; Subramani et al., 2018). Several techniques can be employed to nanostructure surfaces, allowing them to mimic the morphology of living tissue (Long and Rack, 1998), including chemical etching (Klokkevold et al., 1997), ion implantation (De Maezter et al., 2003), or anodic oxidation (Matykina et al., 2007), which are accessible to enhance and modify the surface chemistry of an implant. Among all these techniques, anodic oxidation is a simple way to modify the surface of the titanium and its alloys by the formation of TiO₂ nanotube (TNT) layers in F-containing electrolytes (Macak and Schmuki, 2006; Tsuchiya et al., 2007). Their exceptional features include a large surface area, unique surface chemistry, and low cytotoxicity, the combination of these factors has a beneficial impact on cellular adhesion (Park et al., 2009; Roy et al., 2011). The morphology of TNT layers can be easily manipulated by adjusting both the anodizing voltage and the electrolyte composition (Macak et al., 2008; Lee et al., 2014). Nevertheless, elements from electrolytes, such as F species, are also retained within the TNT layers and cause toxicity issues (Motola et al., 2020).

Early studies on the anodization of TiAlV alloys have demonstrated the formation of TNT layers on the alloy's surface (Macak et al., 2005; Luo et al., 2008). However, the α and β phases of the alloy have different (moderate) dissolution and nanotube formation rates in the anodization electrolyte, resulting in a thickness difference in the TNT layer formed on each phase. The β -phase, enriched in V, dissolves more easily, resulting in thinner nanotube layers than the nanotube layers obtained on the α -phase (Macak et al., 2005; Matykina et al., 2011).

Several studies have reported on the impact of nanostructured surfaces on the growth of different types of cells (Nune et al., 2018; Im et al., 2022), promoting bone-implant integration by providing more surface area for cellular adhesion. In other words, the TiAlV alloy surfaces that were first anodized, having a TNT layer on top, showed better cellular responses such as adhesion, morphology, differentiation, mineralization, and cell seeding rate compared to the bare TiAlV alloy. A recent study of TNT layers with different diameters of nanotubes formed via anodization on TiAlV alloy shows how the adhesion and differentiation of cells can be easily controlled (Filova et al., 2015). Therefore, anodization seems to be a

promising technique to enhance the osseointegration of implants. However, these studies have not emphasized the negative impact of the toxicity of F- and V-species on the biocompatibility of these TNT layers. According to the literature, TiAlV alloy implants can release V-based species into the body, causing adverse health effects (Szewczenko et al., 2010; Vaithilingam et al., 2016). Biologically, the role of V in living mammals, particularly in humans, remains a topic of controversy, with conflicting data regarding its biological activity and toxicity (Goc, 2006; Korbecki et al., 2015). *In vivo* studies suggest that V can accumulate in certain organs, including the liver, and lower concentrations in the kidneys, bones, and spleen (Goc, 2006). Concerning metallic implants that incorporate V, such as TiAlV alloy, Gomes et al. (2011) proposed that V-based species could potentially cause genetic damage, such as DNA breakage.

A possible solution to this problem is a shading of V and other undesirable elements that could compromise biocompatibility properties. Atomic Layer Deposition (ALD) is an effective technique to prepare homogeneous coatings with precise thickness control even in the low nm and sub-nm range (Zazpe et al., 2016). Our previous works (Motola et al., 2020; Baishya et al., 2023; Capek et al., 2024), showed that such ultrathin TiO₂ ALD coating on top of TNT layers on Ti foils and TiAlV alloy foils results in shading of unwanted species, such as F- and V-based species, improving the biocompatibility of the materials without changing their surface morphology (Motola et al., 2020; Baishya et al., 2023; Capek et al., 2024). Several studies have described the antimicrobial activity of TiO₂ ALD coatings, showing that modifying nanomaterial surfaces using TiO₂ ALD coating can inhibit bacterial and yeast biofilm formation (Pessoa et al., 2017; Darwish et al., 2019; González et al., 2021). Nevertheless, a comprehensive approach with analyses that address the surface characteristics (i.e., wettability, roughness, composition, crystallinity, and biocompatibility) of smooth and anodized TiAlV alloy materials before and after ultrathin TiO₂ coating via ALD is still lacking.

To address this gap and to understand the effects of V- and F-based species released from TiAlV alloy implants the effect of ultrathin TiO₂ ALD coatings on the biocompatibility of TiAlV alloy foils and amorphous TNT layers on TiAlV alloy foils was evaluated in this work. At first, TNT layers with different diameters were grown on TiAlV alloy by anodization. The TiO₂ ALD coatings were prepared on part of TNT layers using 1 and 5 ALD cycles, resulting in a nominal coating thickness of ~0.055 and ~0.3 nm, respectively. The cell growth and the cell mechanics, cytoskeleton structure, and adhesion on these ALD-coated compared to non-coated surfaces were evaluated using MG-63 osteoblastic cells and incubation times up to 96 h. The morphology, crystallinity, surface roughness, and wettability of the complete set of materials were assessed using SEM, XPS, static water contact angle (WCA), and Atomic Force Microscopy (AFM). Subsequently, fluorescence microscopy was employed to analyze cell growth on all evaluated materials.

2 Experimental details

2.1 Synthesis and characterization of materials

The TiAlV alloy foils (Goodfellow, 0.1 mm thick, grade 5) were cut into square pieces (1.5 × 1.5 cm²), degreased via sonication in

TABLE 1 Overview of TiAlV foils and TNT layers evaluated in this study.

Structures	Surface modification	Abbreviation used in the text
Foils	-	TiAlV
	1 TiO ₂ ALD cycle	TiAlV + 1c TiO ₂
	5 TiO ₂ ALD cycle	TiAlV + 5c TiO ₂
Nanotubes	TNT layers, diameter ~15 nm	TNT15
	TNT layers, diameter ~15 nm + 1 TiO ₂ ALD cycle	TNT15 + 1c TiO ₂
	TNT layers, diameter ~15 nm + 5 TiO ₂ ALD cycle	TNT15 + 5c TiO ₂
	TNT layers, diameter ~50 nm	TNT50
	TNT layers, diameter ~50 nm + 1 TiO ₂ ALD cycle	TNT50 + 1c TiO ₂
	TNT layers, diameter ~50 nm + 5 TiO ₂ ALD cycle	TNT50 + 5c TiO ₂

acetone and isopropanol in an ultrasonic bath for 1 min, respectively, and then dried in air. TNT layers were prepared via electrochemical anodization of TiAlV foils; with the growth process taking place at room temperature in a glycerol-based electrolyte containing 50 vol% water and 0.27 M NH₄F at 3.3 V or 15 V for 3 h, resulting in TNT layers with an inner nanotube diameter of ~15 and ~50 nm in average, respectively. A Pt foil was used as a counter electrode during the process. A high-voltage potentiostat (HEIDEN, EA-PSI 9200-15, Germany) attached to a digital multimeter (Keithley 2100, United States) was used for voltage control. After anodization, the TNT layers were cleaned by sonication in isopropanol for 5 min and dried in air. The TNT layers are further noted as TNT15 and TNT50 layers.

A part of the TiAlV foils and TNT layers were coated by ultrathin TiO₂ coatings using Atomic Layer Deposition (ALD, TFS200, Beneq). The process was carried out at 300 °C using TiCl₄ (electronic grade 99.9998%, STREM) as the Ti precursor and Milli-pore deionized water (18 MΩ) as the oxygen source. High-purity N₂ (99.9999%) was the carrier and purging gas at a flow rate of 400 standard cubic centimeters per minute (scm). Under these deposition conditions, one ALD growth cycle was defined by the following sequence: TiCl₄ pulse (500 ms)–N₂ purge (3 s)–H₂O pulse (500 ms)–N₂ purge (4 s). The corresponding layers are later denoted as “+ 1c TiO₂” and “+ 5c TiO₂”. The nominal thicknesses of 1c and 5c TiO₂ are ~0.055 and ~0.3 nm, respectively, according to our previous studies (Baishya et al., 2023; Capek et al., 2024). Table 1 provides an executive summary of the TiAlV foils and TNT layers examined in this study.

The surface morphology of all TNT layers and foils was characterized using Scanning Electron Microscopy (FE-SEM, JEOL, JSM 7500 F). The dimensions of the TNT layers were evaluated by statistical analyses of SEM images using proprietary Nanomeasure software.

The surface chemical composition of all TiAlV foils and TNT layers was assessed by X-ray Photoelectron Spectroscopy (XPS, ESCA 2SR, Scienta Omicron) using a monochromatic Al Kα (1486.7 eV) X-ray source. The X-ray source was operated at 250 W. The binding energy scale was referenced to adventitious carbon (284.8 eV). No charging neutralizer was used during the measurements. The spectra were fitted using Shirley-type background by CasaXPS software. The quantitative analysis was

performed using the elemental sensitivity factors provided by the manufacturer.

The wettability was evaluated by measuring the static water contact angle (WCA) using a Surface Energy Evaluation System device (See System E, Advex Instruments) with proprietary image analysis software. WCAs were measured at room temperature, with 3 μL droplets of DI water deposited onto the material's surface, allowing 5 s for stabilization. The contact angles of the water droplets were determined through the tangent line analysis method. Measurements were performed at 5 different positions on each material. All results were expressed as mean ± standard deviation (SD). The contact angle measurements were carried out on as-produced materials without further cleaning or pretreatment (nanotubes after anodization and washing, ALD samples after ALD processes, and foils as delivered). This strategy was used to prevent any uncontrolled and uneven modification of surfaces, particularly to maintain the same chemistry of the surfaces for the subsequent cell tests.

The roughness of TiAlV foils and TNT layers was determined by Atomic Force Microscopy (AFM, Bruker Dimension FastScan) on an area of 5 × 5 μm². Scanasyst-Air tips (fo = 70 kHz) were used.

2.2 Cell culture

Human osteoblast-like cells MG-63 (ATCC No. CRL-1427; doubling time, DT = 31 h) were cultured in Minimum Essential Medium (Merck) with 10% (v/v) fetal bovine serum (Gibco), 2 mmol.L⁻¹ glutamine, 1% non-essential amino acids solution, and 50 μg.mL⁻¹ penicillin/streptomycin solution (Gibco), followed by incubation in an atmosphere of 5% CO₂ at 37 °C. Cells were proven to be mycoplasma-free, and STR analysis confirmed the origin of all cell lines.

2.3 Cell growth on tested materials

The square-shaped substrates were cut into round shapes with a diameter of approx. 5 mm (using sharp scissors). All tested materials were sterilized in 70% ethanol for 30 min, washed with deionized water, and dried. Then, the foils were placed on eight-well chamber

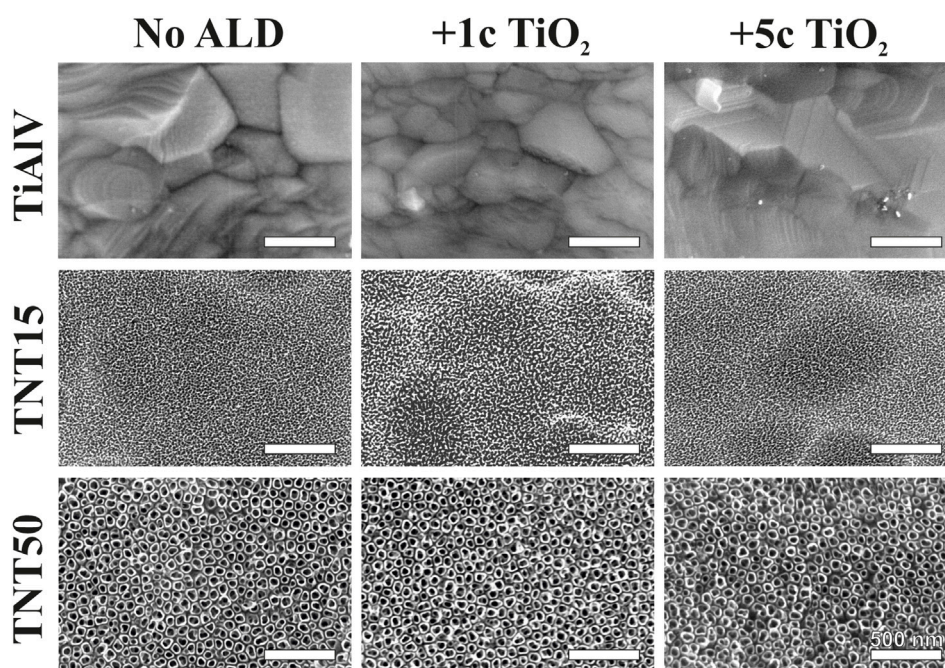


FIGURE 1
SEM top-view images of TiAlV foils, TNT15, and TNT50 layers before and after 1c and 5c TiO₂ ALD.

slides. MG-63 cells at a density of 2×10^3 cells/cm² were seeded in each well of a chamber slide and cultured for 24, 48, 72, and 96 h. Cell counts were established to maintain optimal cultivation densities up to 96 h (the doubling time of the MG-63 cells was 31 h). Phalloidin-FITC and Hoechst 33,258 dyes were used to visualize actin filaments and cell nuclei, respectively. After cell culture for 24, 48, 72, and 96 h, cells were fixed with 3.7% formaldehyde (5 min; 37 °C; dark) and permeabilized with 0.1% Triton X-100 (15 min; 37 °C; dark). Then, 100 μL of phalloidin-FITC ($1 \mu\text{mol.L}^{-1}$) was added and the samples were incubated at 37 °C. After 30 min of phalloidin-FITC loading, 10 μL of Hoechst 33,258 solution was added to cells. The final concentration of Hoechst 33,258 in a well was $2 \mu\text{g.mL}^{-1}$. After 10 min, the cells were washed twice with phosphate-buffered saline (37 °C). Actin filaments (FITC filter, 480/30 nm) and cell nuclei (DAPI filter, 375/28 nm) were observed with an Eclipse 80i fluorescence microscope (Nikon, Japan). The number of cells grown on the surface was counted from at least 35 fields of view using NIS-Elements AR (Nikon, Japan). All experiments were performed at least three times independently. The number of cell nuclei was related to 1 mm² and expressed as mean \pm standard error of the mean (SEM) taken from fluorescence images. Quantitative analysis of cells' elongation on tested samples was provided using NIS-Elements AR (Nikon, Japan).

2.4 Statistics

All cellular experiments were repeated at least three times independently. The number of estimated fields of view was ($n = 35$). The results are expressed as (mean \pm SD). Statistical significance

was analyzed after normality testing using a one-way ANOVA test followed by the Bonferroni posttest (OriginPro 9.0.0, United States) to compare results with each other at a significance level $p = 0.05$.

3 Results and discussion

3.1 Surface, structure, and composition characteristics

Figure 1 shows the representative top-view SEM images of all TiAlV foils and TNT layers before and after 1c and 5c TiO₂ ALD coating. Self-organized TNT layers were obtained on TiAlV foils after the anodization. Detailed measurements revealed an inner diameter of ~ 15 nm after anodization at 3.3 V (TNT15) and ~ 50 nm after anodization at 15 V (TNT50). No significant morphological differences were observed before and after 1c and 5c TiO₂ ALD coating on TiAlV foils and TNT layers by SEM as the nominal thickness of the 1c and 5c TiO₂ ALD coating is extremely small (approx. ~ 0.055 and ~ 0.3 nm, respectively) (Motola et al., 2020).

Figure 1 represents only the anodized α phase of the alloy, while in Supplementary Figure S1 the as-anodized α and β phases are depicted. Nevertheless, α -phase covers approximately 90% of the surface. It is worth noting that the TNT layers reflect the alloy's two-phase nature. However, as this behavior is consistent across all samples, it can neither be altered, nor controlled, thus it does not raise concerns for our research. The thicknesses of the TNT15 and TNT50 layers before 1c and 5c TiO₂ ALD coating are shown in Supplementary Figure S2, and the values determined from SEM cross-sectional images were ~ 118 nm and ~ 410 nm, respectively.

TABLE 2 Surface chemical composition in atomic % before and after 1c TiO₂, and 5c TiO₂ ALD coating, on TiAlV foils, TNT15, and TNT50 layers, measured by XPS.

Chemical composition (atomic %)								
Substrate	C	O	N	F	Ti	Al	V	other
TiAlV	28.1	43.89	4.07	-	16.67	4.44	*	2.83
TiAlV + 1c TiO ₂	18.63	47.38	5.21	-	19.66	3.83	*	5.27
TiAlV + 5c TiO ₂	19.64	49.34	3.85	-	19.08	3.23	*	4.87
TNT15	25.13	46.53	1.74	9.34	13.61	2.84	0.71	0.12
TNT15 + 1c TiO ₂	23.63	50.67	1.03	4.39	17.19	2.61	0.48	-
TNT15 + 5c TiO ₂	21.83	52.87	0.95	3.88	18.06	1.96	0.39	0.06
TNT50	31.92	38.46	2.56	15.57	8.46	2.47	0.54	-
TNT50 + 1c TiO ₂	24.65	50.93	1.1	2.81	17.94	2.08	0.49	-
TNT50 + 5c TiO ₂	23.51	53.98	-	2.09	18.41	1.63	0.38	-

* V was not detected due to its too-low content in the native TiO₂ oxide on the TiAlV foils.

The surface composition in atomic % was assessed through XPS, with the outcomes given in detail in Table 2. Variances in surface atomic composition were observed between uncoated TiAlV foils and those coated with 1c and 5c TiO₂ ALD, as well as between TNT15 and TNT50 layers. Across all 1c and 5c TiO₂ ALD-coated TNT layers, the levels of F and N, originating from anodization electrolytes, as well as V and Al, originating from the alloy, decreased. The V was not detectable on the surface of TiAlV foils, which can be explained by its very low content in the native oxide grown on the alloy upon atmospheric influence. In an earlier work (Macak et al., 2005), once sputtering of the alloy surface was conducted, V species could be clearly detected. However, the V was detected as part of the mixed Ti-Al-V oxide on the TNT layers, the amount decreased with the increment of ALD cycles. This can be explained by the fact that TiO₂ is shading the mentioned elements. On the other hand, C (adventitious carbon) exhibited no significant change after 1c and 5c TiO₂ ALD coating due to its appearance in the environment.

Additionally, the contents of O and Ti increased by adding 1c and 5c TiO₂ ALD. Simultaneously, the ratio between O and Ti changed after the TiO₂ ALD coating (i.e., the ratio gets closer to 2:1), which is clear evidence of the high purity of TiO₂ ALD coatings (Albu et al., 2008; Capek et al., 2024). The reason can be attributed to the uniform TiO₂ coating, achieved through a robust ALD protocol that ensures sufficient precursors and time for the growth of a TiO₂ uniform layer (Motola et al., 2020).

3.2 Wettability measurements

Table 3 and Supplementary Figure S3 present the WCA values and photographs, respectively, for all materials, before and after 1c and 5c TiO₂ ALD coatings. As-prepared TNT layers on TiAlV alloy show a hydrophilic behavior due to the formation of hydroxylated TNT layers. This agrees with the results reported by Shin et al. on anodized TiAlV surfaces using F-containing electrolytes (Shin et al., 2011). Nevertheless, after TiO₂ ALD coating, the TNT layers possess significantly higher contact angles, yielding a somewhat more

TABLE 3 Water contact angles before and after 1c TiO₂, and 5c TiO₂ ALD coating on TiAlV foils, TNT15, and TNT50 layers.

Substrate	No ALD	+1c TiO ₂	+5c TiO ₂
TiAlV	74.9° ± 3.5°	71.1° ± 3.2°	69.0° ± 2.4°
TNT15	17.0° ± 0.5°	90.9° ± 2.6°	101.5° ± 2.0°
TNT50	24.8° ± 3.4°	55.5° ± 1.9°	78.2° ± 2.0°

hydrophobic nature compared to the uncoated TNT layers (Balaur et al., 2005). In fact, according to the literature, the surface wetting properties are influenced by two parameters: surface free energy (SFE) and surface roughness (Neumann and Good, 1972; Giljean et al., 2011). All elements present on the surface of investigated samples exhibit distinct SFE values. Therefore, when WCA measurements are performed on TNT layers formed on TiAlV alloy and modified with TiO₂ ALD coating, the water's bonding tendency relies on the SFE of the elements on the surface that contact the water. This can affect the WCA, making the surface area in contact with water smaller, when the elements exhibit a lower SFE (Neumann and Good, 1972; Yuan and Lee, 2013). As a result, the surfaces of TNT15 and TNT50 layers became more hydrophobic after the TiO₂ ALD coating, with the 5c TiO₂ ALD-coated TNT15 layer showing the highest WCA values among the TNT layers.

On the other hand, the WCA of non-anodized TiAlV foil surfaces was ~74.9° due to the low surface free energy present on this alloy consisting of Ti, Al, and V (Neumann and Good, 1972). The deposition of 1c and 5c TiO₂ ALD coatings on TiAlV foils resulted in slightly enhanced hydrophilic properties of the surfaces, as evidenced by the lower WCA values observed for all foils. In this case, the result is due to the smoothening of the original surface that the TiAlV foils present after the TiO₂ ALD process. The literature also reported a decrease in the contact angle of TiO₂ surfaces after the TiO₂ ALD coating (Liu et al., 2017). Overall, this behavior indicates that the wettability is influenced not only by the surface chemistry (with and without ALD coating) but also by the roughness of surfaces, as shown in the literature (Anselme et al., 2000; Basiaga et al., 2017) and as discussed further.

TABLE 4 Roughness of TiAlV foils, TNT15, and TNT50 layers before and after 1c TiO₂ and 5c TiO₂ ALD coating, respectively.

RMS roughness (nm)			
Substrate	No ALD	+1c TiO ₂	+5c TiO ₂
TiAlV	54.6 ± 17.3	42.8 ± 14.4	39.5 ± 10.5
TNT15	76.1 ± 15.6	82.8 ± 34.5	88.7 ± 32.9
TNT50	64.9 ± 25.0	73.8 ± 9.4	74.8 ± 13.2

3.3 Surface topography and roughness

The roughness of the TiAlV foils and TNT layers was obtained by AFM measurements. Table 4 shows the root means square (RMS) values representing the roughness deviation calculated for each set of materials. A decrease in the RMS values among TiAlV foils was observed with the increasing TiO₂ ALD coating thickness. The TiAlV alloy presents a smoother surface compared with the Ti foils presented in our previous studies (Baishya et al., 2023; Capek et al., 2024). This can be related to the different processing techniques, such as rolling, annealing, or other heat treatments, that may be applied to TiAlV and Ti foils, resulting in variations in surface roughness (Wittenauer and Walsler, 1990; Wang et al., 2019). On the contrary, the roughness of TNT layers increased after ALD coating in all cases. This increase can be attributed to a combination of surface nucleation effects inherent to the ALD technique (Wind et al., 2009; Puurunen et al., 2011), and mechanical interactions (Zazpe et al., 2016; Baishya et al., 2023). A slight roughness difference among the TNT layers with different diameters can be distinguished and in all cases (whether without or with TiO₂ ALD coating), the measured roughness was larger for 15 nm TNT layers. These trends are in good correlation with our previous studies on Ti foils (Motola et al., 2020; Capek et al., 2024).

The AFM topographical image scans before and after 1c and 5c TiO₂ ALD coating of TiAlV foils, TNT15, and TNT50 layers are shown in Supplementary Figure S4, S5. One can see that no metallic grains are visible on the surface of TiAlV foils and TNT layers. The remnant grooves, or grain boundaries have disappeared on substrates containing TNT layers after the anodization process (i.e., formation and dissolution of TiO₂ by the voltage-induced etching of the TiAlV alloy by fluoride ions) (Macak et al., 2005; Motola et al., 2020). Overall, the ALD coating did not detectably change the morphology of all materials, as visualized by the AFM.

3.4 Cell growth and proliferation

An evaluation of the cell growth, i.e., their adhesion and proliferation, of MG-63 cells during incubation up to 96 h was carried out on TiAlV foils, TNT15, and TNT50 layers with and without 1c and 5c TiO₂ ALD coating. In the present study, the MG-63 cell line was used, because this type of cell has been frequently used to evaluate cell growth on surfaces modified by the ALD technique (Motola et al., 2020; Nazarov et al., 2022). This study follows our previous works evaluating the biological effects of TiO₂ ALD coating on nanomaterials (Motola et al., 2020; Capek et al.,

2024). The short-term cultivation effect of TiAlV foils, TNT15, and TNT50 layers coated by 1c and 5c TiO₂ ALD on cell adhesion and proliferation was assessed in this work. Several previous studies evaluated long-term performance in an environment similar to body fluids (Grigal et al., 2012; Abbass et al., 2018). A study by Abbass et al. (2018) proved the corrosion resistance and low toxicity of the material coated by TiO₂ ALD in long-term incubation (2 weeks) in the simulated body fluid. This is also confirmed by another study (Grigal et al., 2012), where the stability of the amorphous TiO₂ coating was better compared to the anatase phase. Figure 2 shows photomicrographs of MG-63 cells cultured on TiAlV foils, TNT15, and TNT50 layers, which were uncoated or coated with 1c or 5c TiO₂ ALD. To identify the functional morphology of MG-63, staining of cell nuclei and actin filaments with fluorescent probes was used according to other authors (Iwata et al., 2017; Li et al., 2020). Subsequently, the images were subjected to image analysis. Cell nuclei were counted in individual fields of view and related to an area (=mm²), which is also a common approach for the quantification of cell growth in other studies (Kim et al., 2005; Zhang et al., 2012). Figure 3 shows an increased number of cells in all 1c and 5c TiO₂ ALD-coated materials (TiAlV foils, TNT15, and TNT50 layers), compared to their uncoated counterparts at all time intervals. The highest increases in cell densities were observed in both TiAlV foils and TNT15 layers with 1c and 5c TiO₂ ALD coating, compared to the uncoated ones after 96 h. As the doubling time of the MG-63 cells was 31 h, it can be assumed that the TiO₂ coating had a beneficial effect not only on the cell adhesion but also on the cell proliferation. Other reports used a wide range of TiO₂ ALD film thicknesses achieved by a range of ALD cycles, i.e., 1-250c (Motola et al., 2020; Capek et al., 2024), 250-1000c (Huang et al., 2019), and more than 1000c TiO₂ (Huang et al., 2019).

WCA measurements shown in Table 3 provided findings of decreased hydrophilicity for all coated TNTs (i.e., 1c and 5c TiO₂ ALD) compared to uncoated ones. In the case of the TiAlV foil, the wettability remained more or less unchanged after TiO₂ ALD coatings. To ensure the cell adhesion to a surface, the optimal range of water contact angles has been reported in several studies to be between 60° and 80° (Arima and Iwata, 2007; Kim et al., 2007; 2015; Lv et al., 2015; Yao et al., 2019). Our results showed that WCA in both tested TNTs after 1c and 5c TiO₂ ALD reached values nearer to the optimal range of 60°–80° in comparison to WCA values of uncoated TNTs. However, WCA is not the only factor influencing cell growth, the whole situation is more complex. The number of MG-63 cells cultured on uncoated TiAlV foils (as such or with TNT layers) was lower compared to coated counterparts with 1c and 5c TiO₂ ALD, as shown in Figures 2, 3. In particular, the increased cell number can be assigned to the reduction of the cytotoxic effect of V and F elements that are present on the uncoated surfaces. In samples coated with 1c and 5c TiO₂ ALD, the concentrations of V and F elements were reduced (as demonstrated by XPS results in Table 2) due to the shading effect that TiO₂ ALD coating gives to the surfaces and thus their cytotoxic effect was reduced. This effect was already described in the literature, either as the negative effect of V and F elements on the cell proliferation (Goc, 2006; Szweczenko et al., 2010), or the possible involvement of V and its compounds in the induction of the formation of ROS, which can suppress cell growth (Cortizo et al., 2000; Aureliano et al., 2023).

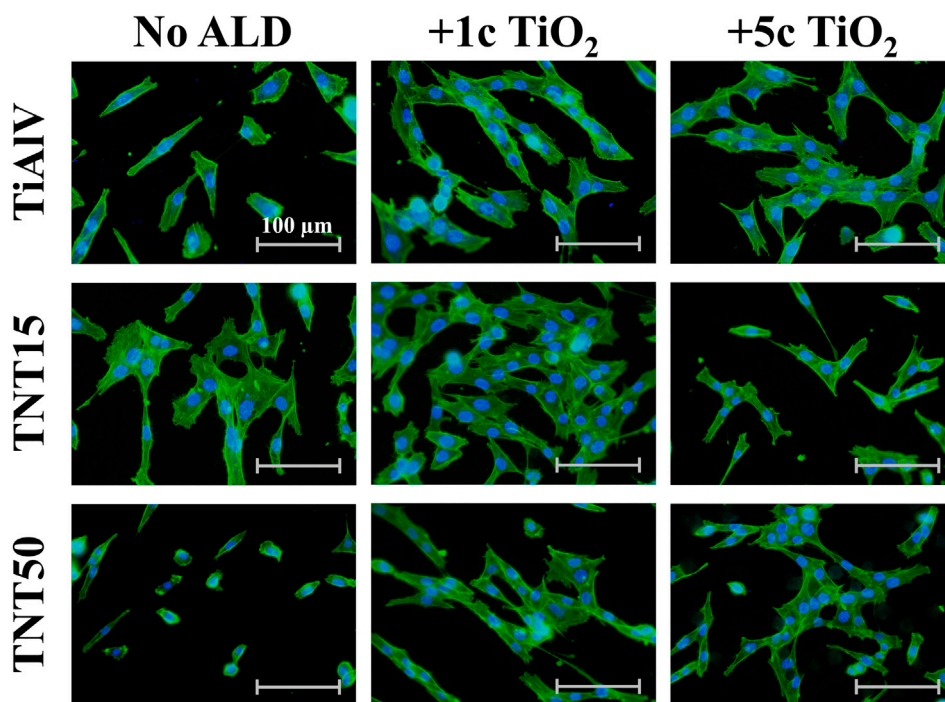


FIGURE 2 Photomicrographs of MG-63 cells grown on uncoated or 1c and 5c TiO₂ ALD-coated TiAlV foils, TNT15 and TNT50 layers for 72 h (No ALD = without TiO₂ ALD coating; 1c ALD = 1c TiO₂ ALD coating; 5c ALD = 5c TiO₂ ALD coating). The actin filaments were stained with the Phalloidin-FITC probe (green), and the cell's nuclei were stained with the Hoechst 33,258 probe (blue).

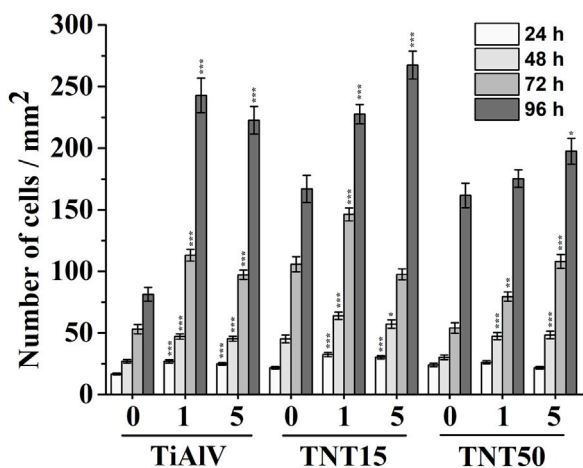


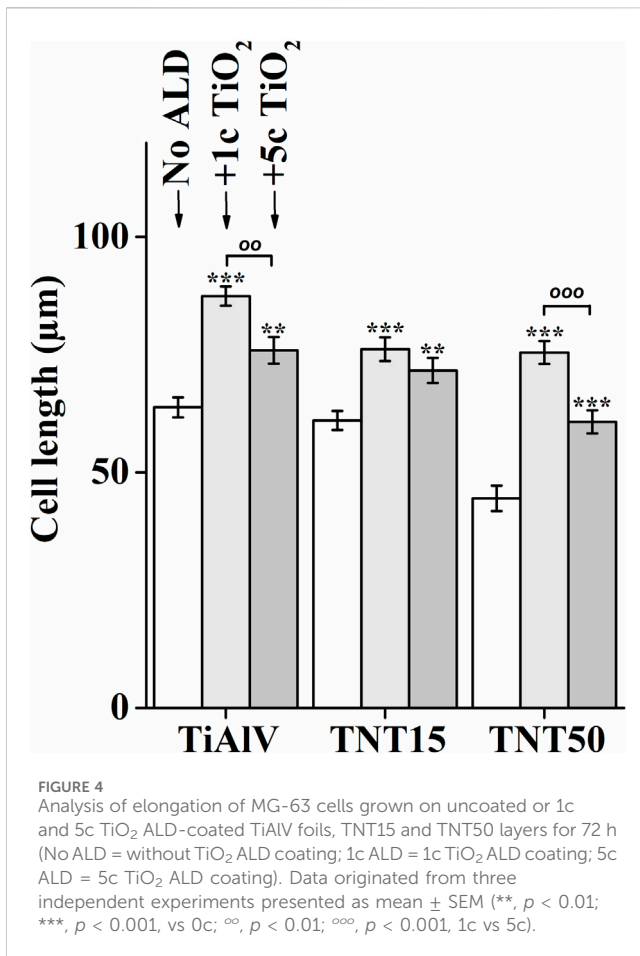
FIGURE 3 Density of MG-63 cells grown on uncoated or 1c and 5c TiO₂ ALD-coated TiAlV foils, TNT15 and TNT50 layers for 24–96 h (0 = without TiO₂ ALD coating; 1 = 1c TiO₂ ALD coating; 5 = 5c TiO₂ ALD coating). Data originated from three independent experiments presented as mean ± SEM (*, $p < 0.05$; **, $p < 0.01$; ***, $p < 0.001$, vs 0c at appropriate time interval).

3.5 Cell elongation

The cell elongation was evaluated from photomicrographs obtained (examples of which are given in Figure 2), as it

correlates with increased adhesion of cells to a material (Motola et al., 2020; Nazarov et al., 2022). Figure 4 shows the resulting analysis of the elongation of MG-63 cells incubated for 72 h on TiAlV foils, TNT15, and TNT50 layers with and without 1c and 5c TiO₂ ALD coating. Cells cultured in TiAlV foils and TNT layers with TiO₂ ALD coatings had a more elongated structure, compared to those cultured in uncoated samples. An increase in elongation by approximately 20% was observed in cells cultured on TiAlV foils, TNT15, and TNT50 layers coated with 1c and 5c TiO₂ ALD compared to uncoated samples. Interestingly, cells grown on TiAlV foils and TNT50 layers coated with 1c TiO₂ ALD had a significantly increased elongated structure compared to materials coated with 5c TiO₂ ALD. The increase in the elongation in cells on TiO₂ ALD coated materials compared to uncoated materials can be attributed to the achievement of WCA values in the optimal range of 60°–80°. The difference in the elongation of cells grown on 1c and 5c TiO₂ ALD coated materials could be likely ascribed to the combined effects of differing wettability and surface structure and chemistry, according to AFM and XPS results. The photomicrographs of MG-63 cells after 24, 48, and 96 h are provided as supplementary data in Supplementary Figures S6–S8, and the evaluation of elongation in MG-63 cells grown on TiAlV foils, TNT15, and TNT50 layers for 24 and 48 h is provided as supplementary data in Supplementary Figure S9. MG-63 cell elongation analysis was not performed in the 96-h time interval due to the high cell confluence that is nearly 100%.

The increased number of elongated cells after cultivation on materials modified by TiO₂ ALD was also observed in several studies by other authors (Chuang et al., 2021; Abushahba et al., 2023). For



instance, the elongated structure of human dental pulp stem cells was observed after culture on Si substrates coated with 50c TiO₂ after 24 h. The cells grown on ALD-modified Si substrates exhibited higher average aspect ratios (i.e., ratio of the cellular major and minor axes) compared to unmodified materials (Chuang et al., 2021). The MC3T3-E1 osteoblasts growth on Ti sheets with ALD coating have been studied in the literature (Kylmäoja et al., 2022; Abushahba et al., 2023), showing an elongated structure for instance with/without 4000 cycles of hydroxyapatite coating were assessed after 48 h (Kylmäoja et al., 2022). Cells on hydroxyapatite-coated Ti sheets had higher average aspect ratios compared to uncoated Ti sheets. For cells grown on Ti sheets, a circular structure was detected in the contrast to cells grown on Ti sheets coated with hydroxyapatite having elongated morphology.

4 Conclusion

The influence of the surface morphology and chemical composition of TiAlV foils and TNT layers grown on TiAlV foils on the cell growth of MG-63 osteoblastic cells before and after 1c or 5c TiO₂ ALD coating was investigated for the first time. The addition of ultrathin TiO₂ ALD coatings improved the biocompatibility of TNT layers for the cell growth. All the surfaces were evaluated in terms of morphology, composition, and wettability. SEM images did not show any significant changes

in the morphology of surfaces after 1c and 5c TiO₂ ALD coating in any of the substrates. However, XPS analysis revealed that the chemical composition of all surfaces changed after 1c and 5c TiO₂ ALD coating, resulting in a decrease in the occurrence of F and V elements. WCA results demonstrated that the surface remained stably hydrophilic for TiAlV foils after 1c and 5c TiO₂ ALD coating, contrary to the case of TNT layers, when the WCA strongly increased after 1c and 5c TiO₂ ALD coating towards more hydrophobic character. The change of WCA was probably caused by changes in the surface free energy and the roughness after TiO₂ ALD coatings. The AFM results showed a significant increase in the roughness after TiO₂ ALD coating on all TNT layers, but for the TiAlV foils the roughness did not change very significantly. In terms of the biocompatibility, the growth of MG-63 cells on all materials was estimated. The cell growth evaluation showed a significant increase in the number of cells cultivated on TiAlV foils, TNT15 or TNT50 layers coated with 1c or 5c TiO₂ ALD, in comparison to uncoated samples. These outcomes were supported by findings of elongated cells cultured on all tested 1c or 5c TiO₂ ALD coated materials demonstrating more beneficial circumstances for cell growth after 1c or 5c TiO₂ ALD coating. This effect is ensured by the combination of F and V shading and achievement of WCA values near the range of 60°–80° being optimal for the cell adhesion to a surface in general. Overall, the results presented here bring new and very valuable findings, on how to increase the biocompatibility of TiAlV-derived materials using ultra-thin TiO₂ ALD coating, although additional detailed cellular studies are required to describe the exact mechanism accounting for the increased proliferation of MG63 cells.

Data availability statement

The original contributions presented in the study are included in the article/Supplementary Material, further inquiries can be directed to the corresponding authors.

Author contributions

MS: Writing–review and editing, Writing–original draft, Methodology, Investigation, Conceptualization. JC: Writing–review and editing, Writing–original draft, Methodology, Investigation, Conceptualization. KB: Writing–review and editing, Investigation. JR-P: Writing–review and editing, Investigation. JB: Writing–review and editing, Investigation. SJ: Writing–review and editing, Investigation. RZ: Writing–review and editing, Investigation. HS: Writing–review and editing, Investigation. TR: Writing–review and editing, Supervision, Methodology, Funding acquisition. JM: Writing–review and editing, Supervision, Methodology, Funding acquisition, Conceptualization.

Funding

The author(s) declare that financial support was received for the research, authorship, and/or publication of this article. The authors were supported by the Ministry of Education, Youth and Sports of

the Czech Republic projectS LM2023037, LM2023051 and CZ.02.1.01/0.0/0.0/17_048/0007421).

Acknowledgments

The authors gratefully acknowledge support from the Ministry of Education, Youth and Sports of the Czech Republic for supporting the large research infrastructure CEMNAT (LM2023037) and CzechNanoLab (LM2023051) and also to project NANOBIO (nr. CZ.02.1.01/0.0/0.0/17_048/0007421).

Conflict of interest

The authors declare that the research was conducted in the absence of any commercial or financial relationships that could be construed as a potential conflict of interest.

The author(s) declared that they were an editorial board member of Frontiers, at the time of submission. This had no impact on the peer review process and the final decision.

References

- Abbass, M. K., Ajeel, S. A., and Wadullah, H. M. (2018). "Biocompatibility, bioactivity and corrosion resistance of stainless steel 316L nanocoated with TiO₂ and Al₂O₃ by atomic layer deposition method," in *Journal of physics: conference series* (Bristol, United Kingdom: IOP Publishing), 012017.
- Abushahba, F., Areid, N., Kylmäoja, E., Holopainen, J., Ritala, M., Hupa, L., et al. (2023). Effect of atomic-layer-deposited hydroxyapatite coating on surface thrombogenicity of titanium. *Coatings* 13, 1810. doi:10.3390/coatings13101810
- Albu, S. P., Ghicov, A., Aldabergenova, S., Drechsel, P., LeClere, D., Thompson, G. E., et al. (2008). Formation of double-walled TiO₂ nanotubes and robust anatase membranes. *Adv. Mater.* 20, 4135–4139. doi:10.1002/adma.200801189
- Anselme, K., Linez, P., Bigerelle, M., Le Maguer, D., Le Maguer, A., Hardouin, P., et al. (2000). The relative influence of the topography and chemistry of TiAl₆V₄ surfaces on osteoblastic cell behaviour. *Biomaterials* 21, 1567–1577. doi:10.1016/S0142-9612(00)00042-9
- Arima, Y., and Iwata, H. (2007). Effect of wettability and surface functional groups on protein adsorption and cell adhesion using well-defined mixed self-assembled monolayers. *Biomaterials* 28, 3074–3082. doi:10.1016/j.biomaterials.2007.03.013
- Aureliano, M., De Sousa-Coelho, A. L., Dolan, C. C., Roess, D. A., and Crans, D. C. (2023). Biological consequences of vanadium effects on formation of reactive oxygen species and lipid peroxidation. *Int. J. Mol. Sci.* 24, 5382. doi:10.3390/ijms24065382
- Baishya, K., Vrchovecká, K., Alijani, M., Rodriguez-Pereira, J., Thalluri, S. M., Goldbergová, M. P., et al. (2023). Bio-AFM exploits enhanced response of human gingival fibroblasts on TiO₂ nanotubular substrates with thin TiO₂ coatings. *Appl. Surf. Sci. Adv.* 18, 100459. doi:10.1016/j.apsadv.2023.100459
- Balaur, E., Macak, J. M., Taveira, L., and Schmuki, P. (2005). Tailoring the wettability of TiO₂ nanotube layers. *Electrochem Commun.* 7, 1066–1070. doi:10.1016/j.elecom.2005.07.014
- Basiaga, M., Walke, W., Staszuk, M., Kajzer, W., Kajzer, A., and Nowińska, K. (2017). Influence of ALD process parameters on the physical and chemical properties of the surface of vascular stents. *Archives Civ. Mech. Eng.* 17, 32–42. doi:10.1016/j.acme.2016.08.001
- Campoccia, D., Montanaro, L., and Arciola, C. R. (2006). The significance of infection related to orthopedic devices and issues of antibiotic resistance. *Biomaterials* 27, 2331–2339. doi:10.1016/j.biomaterials.2005.11.044
- Capek, J., Sepúlveda, M., Bacova, J., Rodriguez-Pereira, J., Zazpe, R., Cicmancova, V., et al. (2024). Ultrathin TiO₂ coatings via atomic layer deposition strongly improve cellular interactions on planar and nanotubular biomedical Ti substrates. *ACS Appl. Mater. Interfaces* 16, 5627–5636. doi:10.1021/acsmi.3c17074
- Chen, Q., and Thouas, G. A. (2015). Metallic implant biomaterials. *Mater. Sci. Eng. R Rep.* 87, 1–57. doi:10.1016/j.mser.2014.10.001
- Chuang, Y.-C., Wang, L., Feng, K.-C., Subramanian, A., Chang, C.-C., Simon, M., et al. (2021). The role of titania surface coating by atomic layer deposition in improving

Generative AI statement

The author(s) declare that no Generative AI was used in the creation of this manuscript.

Publisher's note

All claims expressed in this article are solely those of the authors and do not necessarily represent those of their affiliated organizations, or those of the publisher, the editors and the reviewers. Any product that may be evaluated in this article, or claim that may be made by its manufacturer, is not guaranteed or endorsed by the publisher.

Supplementary material

The Supplementary Material for this article can be found online at: <https://www.frontiersin.org/articles/10.3389/fbioe.2024.1515810/full#supplementary-material>

osteogenic differentiation and hard tissue formation of dental pulp stem cells. *Adv. Mater.* 23, 2100097. doi:10.1002/adem.202100097

Cortizo, A. M., Bruzzone, L., Molinuevo, S., and Etcheverry, S. B. (2000). A possible role of oxidative stress in the vanadium-induced cytotoxicity in the MC3T3E1 osteoblast and UMR106 osteosarcoma cell lines. *Toxicology* 147, 89–99. doi:10.1016/S0300-483X(00)00181-5

Costa, B. C., Tokuhara, C. K., Rocha, L. A., Oliveira, R. C., Lisboa-Filho, P. N., and Pessoa, J. C. (2019). Vanadium ionic species from degradation of Ti-6Al-4V metallic implants: *in vitro* cytotoxicity and speciation evaluation. *Mater. Sci. Eng. C* 96, 730–739. doi:10.1016/j.msec.2018.11.090

Darwish, G., Huang, S., Knoernschild, K., Sukotjo, C., Campbell, S., Bishal, A. K., et al. (2019). Improving polymethyl methacrylate resin using a novel titanium dioxide coating. *J. Prosthodont.* 28, 1011–1017. doi:10.1111/jopr.13032

De Maezta, M. A., Alava, J. I., and Gay-Escoda, C. (2003). Ion implantation: surface treatment for improving the bone integration of titanium and Ti6Al4V dental implants. *Clin. Oral Implants Res.* 14, 57–62. doi:10.1034/j.1600-0501.2003.140108.x

Filova, E., Fojt, J., Kryslava, M., Moravec, H., Joska, L., and Bacakova, L. (2015). The diameter of nanotubes formed on Ti-6Al-4V alloy controls the adhesion and differentiation of Saos-2 cells. *Int. J. Nanomedicine* 10, 7145–7163. doi:10.2147/ijn.s87474

Giljean, S., Bigerelle, M., Anselme, K., and Haidara, H. (2011). New insights on contact angle/roughness dependence on high surface energy materials. *Appl. Surf. Sci.* 257, 9631–9638. doi:10.1016/j.apsusc.2011.06.088

Gittens, R. A., Olivares-Navarrete, R., Schwartz, Z., and Boyan, B. D. (2014). Implant osseointegration and the role of microroughness and nanostructures: lessons for spine implants. *Acta Biomater.* 10, 3363–3371. doi:10.1016/j.actbio.2014.03.037

Goc, A. (2006). Biological activity of vanadium compounds. *Cent. Eur. J. Biol.* 1, 314–332. doi:10.2478/s11535-006-0029-z

Gomes, C. C., Moreira, L. M., Santos, V. J. S. V., Ramos, A. S., Lyon, J. P., Soares, C. P., et al. (2011). Assessment of the genetic risks of a metallic alloy used in medical implants. *Genet. Mol. Biol.* 34, 116–121. doi:10.1590/s1415-47572010005000118

González, A. S., Riego, A., Vega, V., García, J., Galié, S., Gutierrez del Rio, I., et al. (2021). Functional antimicrobial surface coatings deposited onto nanostructured 316L food-grade stainless steel. *Nanomaterials* 11, 1055. doi:10.3390/nano11041055

Grigal, I. P., Markeev, A. M., Gudkova, S. A., Chernikova, A. G., Mityaev, A. S., and Alekhin, A. P. (2012). Correlation between bioactivity and structural properties of titanium dioxide coatings grown by atomic layer deposition. *Appl. Surf. Sci.* 258, 3415–3419. doi:10.1016/j.apsusc.2011.11.082

Huang, L., Su, K., Zheng, Y.-F., Yeung, K. W.-K., and Liu, X.-M. (2019). Construction of TiO₂/silane nanofilm on AZ31 magnesium alloy for controlled degradability and enhanced biocompatibility. *Rare Met.* 38, 588–600. doi:10.1007/s12598-018-1187-7

Im, C., Park, J.-H., Jeon, Y.-M., Kim, J.-G., Jang, Y.-S., Lee, M.-H., et al. (2022). Improvement of osseointegration of Ti-6Al-4V ELI alloy orthodontic mini-screws

- through anodization, cyclic pre-calcification, and heat treatments. *Prog. Orthod.* 23, 11. doi:10.1186/s40510-022-00405-8
- Iwata, N., Nozaki, K., Horiuchi, N., Yamashita, K., Tsutsumi, Y., Miura, H., et al. (2017). Effects of controlled micro-/nanosurfaces on osteoblast proliferation. *J. Biomed. Mater. Res. A* 105, 2589–2596. doi:10.1002/jbm.a.36118
- Kim, H. J., Kim, S. H., Kim, M. S., Lee, E. J., Oh, H. G., Oh, W. M., et al. (2005). Varying Ti-6Al-4V surface roughness induces different early morphologic and molecular responses in MG63 osteoblast-like cells. *J. Biomed. Mater. Res. Part A Official J. Soc. Biomaterials, Jpn. Soc. Biomaterials, Aust. Soc. Biomaterials Korean Soc. Biomaterials* 74, 366–373. doi:10.1002/jbm.a.30327
- Kim, S. H., Ha, H. J., Ko, Y. K., Yoon, S. J., Rhee, J. M., Kim, M. S., et al. (2007). Correlation of proliferation, morphology and biological responses of fibroblasts on LDPE with different surface wettability. *J. Biomater. Sci. Polym. Ed.* 18, 609–622. doi:10.1163/156856207780852514
- Kim, T., Sridharan, I., Zhu, B., Orgel, J., and Wang, R. (2015). Effect of CNT on collagen fiber structure, stiffness assembly kinetics and stem cell differentiation. *Mater. Sci. Eng. C* 49, 281–289. doi:10.1016/j.msec.2015.01.014
- Klokkevold, P. R., Nishimura, R. D., Adachi, M., and Caputo, A. (1997). Osseointegration enhanced by chemical etching of the titanium surface. A torque removal study in the rabbit. *Clin. Oral Implants Res.* 8, 442–447. doi:10.1034/j.1600-0501.1997.080601.x
- Konttinen, Y. T., and Pajarinen, J. (2013). Adverse reactions to metal-on-metal implants. *Nat. Rev. Rheumatol.* 9, 5–6. doi:10.1038/nrrheum.2012.218
- Korbecki, J., Baranowska-Bosiacka, I., Gutowska, I., and Chlubek, D. (2015). Vanadium compounds as pro-inflammatory agents: effects on cyclooxygenases. *Int. J. Mol. Sci.* 16, 12648–12668. doi:10.3390/ijms160612648
- Kylmäoja, E., Holopainen, J., Abushabba, F., Ritala, M., and Tuukkanen, J. (2022). Osteoblast attachment on titanium coated with hydroxyapatite by atomic layer deposition. *Biomolecules* 12, 654. doi:10.3390/biom12050654
- Lee, K., Mazare, A., and Schmuki, P. (2014). One-dimensional titanium dioxide nanomaterials: nanotubes. *Chem. Rev.* 114, 9385–9454. doi:10.1021/cr500061m
- Li, Y., Wang, S., Dong, Y., Mu, P., Yang, Y., Liu, X., et al. (2020). Effect of size and crystalline phase of TiO₂ nanotubes on cell behaviors: a high throughput study using gradient TiO₂ nanotubes. *Bioact. Mater.* 5, 1062–1070. doi:10.1016/j.bioactmat.2020.07.005
- Liu, L., Bhatia, R., and Webster, T. J. (2017). Atomic layer deposition of nano-TiO₂ thin films with enhanced biocompatibility and antimicrobial activity for orthopedic implants. *Int. J. Nanomedicine* 12, 8711–8723. doi:10.2147/ijn.s148065
- Long, M., and Rack, H. J. (1998). Titanium alloys in total joint replacement—a materials science perspective. *Biomaterials* 19, 1621–1639. doi:10.1016/s0142-9612(97)00146-4
- Luo, B., Yang, H., Liu, S., Fu, W., Sun, P., Yuan, M., et al. (2008). Fabrication and characterization of self-organized mixed oxide nanotube arrays by electrochemical anodization of Ti–6Al–4V alloy. *Mater. Lett.* 62, 4512–4515. doi:10.1016/j.matlet.2008.08.015
- Lv, L., Liu, Y., Zhang, P., Zhang, X., Liu, J., Chen, T., et al. (2015). The nanoscale geometry of TiO₂ nanotubes influences the osteogenic differentiation of human adipose-derived stem cells by modulating H3K4 trimethylation. *Biomaterials* 39, 193–205. doi:10.1016/j.biomaterials.2014.11.002
- Macak, J. M., Hildebrand, H., Marten-Jahns, U., and Schmuki, P. (2008). Mechanistic aspects and growth of large diameter self-organized TiO₂ nanotubes. *J. Electroanal. Chem.* 621, 254–266. doi:10.1016/j.jelechem.2008.01.005
- Macak, J. M., and Schmuki, P. (2006). Anodic growth of self-organized anodic TiO₂ nanotubes in viscous electrolytes. *Electrochim Acta* 52, 1258–1264. doi:10.1016/j.electacta.2006.07.021
- Macak, J. M., Tsuchiya, H., Taveira, L., Ghicov, A., and Schmuki, P. (2005). Self-organized nanotubular oxide layers on Ti-6Al-7Nb and Ti-6Al-4V formed by anodization in NH₄F solutions. *J. Biomed. Mater. Res. A* 75, 928–933. doi:10.1002/jbm.a.30501
- Magesh, S., Vasanth, G., Revathi, A., and Geetha, M. (2018). “Use of nanostructured materials in implants,” in *Nanobiomaterials* (Elsevier), 481–501.
- Matykina, E., Conde, A., De Damborenea, J., y Marero, D. M., and Arenas, M. A. (2011). Growth of TiO₂-based nanotubes on Ti–6Al–4V alloy. *Electrochim Acta* 56, 9209–9218. doi:10.1016/j.electacta.2011.07.131
- Matykina, E., Monfort, F., Berkani, A., Skeldon, P., Thompson, G. E., and Gough, J. (2007). Characterization of spark-anodized titanium for biomedical applications. *J. Electrochem Soc.* 154, C279. doi:10.1149/1.2717383
- Motola, M., Capek, J., Zazpe, R., Bacova, J., Hromadko, L., Bruckova, L., et al. (2020). Thin TiO₂ coatings by ALD enhance the cell growth on TiO₂ nanotubular and flat substrates. *ACS Appl. Bio Mater* 3, 6447–6456. doi:10.1021/acsabm.0c00871
- Nazarov, D., Ezhov, I., Yuditceva, N., Shevtsov, M., Rudakova, A., Kalganov, V., et al. (2022). Antibacterial and osteogenic properties of Ag nanoparticles and Ag/TiO₂ nanostructures prepared by atomic layer deposition. *J. Funct. Biomater.* 13, 62. doi:10.3390/fb13020062
- Neumann, A. W., and Good, R. J. (1972). Thermodynamics of contact angles. I. Heterogeneous solid surfaces. *J. Colloid Interface Sci.* 38, 341–358. doi:10.1016/0021-9797(72)90251-2
- Nune, K. C., Misra, R. D. K., Gai, X., Li, S. J., and Hao, Y. L. (2018). Surface nanotopography-induced favorable modulation of bioactivity and osteoconductive potential of anodized 3D printed Ti-6Al-4V alloy mesh structure. *J. Biomater. Appl.* 32, 1032–1048. doi:10.1177/0885328217748860
- Oliveira, N. T. C., Ferreira, E. A., Duarte, L. T., Biaggio, S. R., Rocha-Filho, R. C., and Bocchi, N. (2006). Corrosion resistance of anodic oxides on the Ti–50Zr and Ti–13Nb–13Zr alloys. *Electrochim Acta* 51, 2068–2075. doi:10.1016/j.electacta.2005.07.015
- Park, J., Bauer, S., Schlegel, K. A., Neukam, F. W., von der Mark, K., and Schmuki, P. (2009). TiO₂ nanotube surfaces: 15 nm—an optimal length scale of surface topography for cell adhesion and differentiation. *small* 5, 666–671. doi:10.1002/sml.200801476
- Pessoa, R. S., Dos Santos, V. P., Cardoso, S. B., Doria, A., Figueira, F. R., Rodrigues, B. V. M., et al. (2011). TiO₂ coatings via atomic layer deposition on polyurethane and polydimethylsiloxane substrates: properties and effects on C. albicans growth and inactivation process. *Appl. Surf. Sci.* 422, 73–84. doi:10.1016/j.apsusc.2017.05.254
- Puurunen, R. L., Sajavaara, T., Santala, E., Miikkulainen, V., Saukkonen, T., Laitinen, M., et al. (2011). Controlling the crystallinity and roughness of atomic layer deposited titanium dioxide films. *J. Nanosci. Nanotechnol.* 11, 8101–8107. doi:10.1166/jnn.2011.5060
- Roy, P., Berger, S., and Schmuki, P. (2011). TiO₂ nanotubes: synthesis and applications. *Angew. Chem. Int. Ed.* 50, 2904–2939. doi:10.1002/anie.201001374
- Sarraf, M., Rezvani Ghomi, E., Alipour, S., Ramakrishna, S., and Liana Sukiman, N. (2021). A state-of-the-art review of the fabrication and characteristics of titanium and its alloys for biomedical applications. *Bioes. Manuf.* 5, 371–395. doi:10.1007/s42242-021-00170-3
- Shin, D. H., Shokuhfar, T., Choi, C. K., Lee, S.-H., and Friedrich, C. (2011). Wettability changes of TiO₂ nanotube surfaces. *Nanotechnology* 22, 315704. doi:10.1088/0957-4484/22/31/315704
- Singh, R., and Dahotre, N. B. (2007). Corrosion degradation and prevention by surface modification of biometallic materials. *J. Mater. Sci. Mater. Med.* 18, 725–751. doi:10.1007/s10856-006-0016-y
- Subramani, K., Lavenus, S., Rozé, J., Louarn, G., and Layrolle, P. (2018). “Impact of nanotechnology on dental implants,” in *Emerging nanotechnologies in dentistry*, 83–97.
- Szewczenko, J., Walke, W., Nowinska, K., and Marciniak, J. (2010). Corrosion resistance of Ti-6Al-4V alloy after diverse surface treatments. *Materwiss Werkstsch* 41, 360–371. doi:10.1002/mawe.201000610
- Tsuchiya, H., Berger, S., Macak, J. M., Ghicov, A., and Schmuki, P. (2007). Self-organized porous and tubular oxide layers on TiAl alloys. *Electrochem Commun.* 9, 2397–2402. doi:10.1016/j.elecom.2007.07.013
- Vaithilingam, J., Prina, E., Goodridge, R. D., Hague, R. J. M., Edmondson, S., Rose, F. R. A. J., et al. (2016). Surface chemistry of Ti6Al4V components fabricated using selective laser melting for biomedical applications. *Mater. Sci. Eng. C* 67, 294–303. doi:10.1016/j.msec.2016.05.054
- Vasconcelos, D. M., Santos, S. G., Lamghari, M., and Barbosa, M. A. (2016). The two faces of metal ions: from implants rejection to tissue repair/regeneration. *Biomaterials* 84, 262–275. doi:10.1016/j.biomaterials.2016.01.046
- Wang, L., Xie, L., Shen, P., Fan, Q., Wang, W., Wang, K., et al. (2019). Surface microstructure and mechanical properties of Ti-6Al-4V/Ag nanocomposite prepared by FSP. *Mater. Charact.* 153, 175–183. doi:10.1016/j.matchar.2019.05.002
- Wind, R. W., Fabreguette, F. H., Sechrist, Z. A., and George, S. M. (2009). Nucleation period, surface roughness, and oscillations in mass gain per cycle during W atomic layer deposition on Al₂O₃. *J. Appl. Phys.* 105. doi:10.1063/1.3103254
- Wittenauer, J., and Walsler, B. (1990). Processing and properties of titanium foils. *Mater. Sci. Eng. A* 123, 45–52. doi:10.1016/0921-5093(90)90208-k
- Yao, L., Wu, X., Wu, S., Pan, X., Tu, J., Chen, M., et al. (2019). Atomic layer deposition of zinc oxide on microrough zirconia to enhance osteogenesis and antibiosis. *Ceram. Int.* 45, 24757–24767. doi:10.1016/j.ceramint.2019.08.216
- Yuan, Y., and Lee, T. R. (2013). “Contact angle and wetting properties,” in *Surface science techniques* (Springer), 3–34.
- Zazpe, R., Knaut, M., Sopha, H., Hromadko, L., Albert, M., Prikryl, J., et al. (2016). Atomic layer deposition for coating of high aspect ratio TiO₂ nanotube layers. *Langmuir* 32, 10551–10558. doi:10.1021/acs.langmuir.6b03119
- Zhang, W., Li, Z., Liu, Y., Ye, D., Li, J., Xu, L., et al. (2012). Biofunctionalization of a titanium surface with a nano-sawtooth structure regulates the behavior of rat bone marrow mesenchymal stem cells. *Int. J. Nanomedicine* 7, 4459–4472. doi:10.2147/ijn.s33575
- Zhao, J., and Castranova, V. (2011). Toxicology of nanomaterials used in nanomedicine. *J. Toxicol. Environ. Health, Part B* 14, 593–632. doi:10.1080/10937404.2011.615113